Solid Freeform Fabrication 2018: Proceedings of the 29th Annual International Solid Freeform Fabrication Symposium – An Additive Manufacturing Conference
Reviewed Paper

VISCOSITY CONTROL OF PSEUDOPLASTIC POLYMER MIXTURES FOR APPLICATIONS IN ADDITIVE-MANUFACTURING

Apoorv Vaish*, Shien Yang Lee* and Pablo Valdivia y Alvarado*,†

* Engineering Product Development, Singapore University of Technology and Design
† Digital Manufacturing and Design Centre, Singapore University of Technology and Design

Abstract

Various additive manufacturing (AM) processes exploit the rheological properties of non-Newtonian (e.g. pseudoplastic) polymers for stability and feature realization. For embedded 3D-printing (e3DP) and direct ink writing (DIW), features are deposited on top or within a layer of matrix/base material and the rheological properties of the matrix are crucial for satisfactory prints. Due to their high apparent viscosities under static conditions, these base polymers do not flow easily when poured in bulk into the fabrication space. Traditionally, manual methods were employed to spread them into an even layer. In this study, an alternative approach to spread and level pseudoplastic polymers using oscillatory shear stresses generated by a vibrating actuator is presented. The proposed approach lowers the viscosity of the polymers, thereby facilitating gravity-driven flow to generate a flat polymer-air interface. A fluid rheology model detailing the parameters influencing the process is presented and experiments are performed using these parameters.

Introduction

Additive manufacturing (AM) involves sequential (e.g. layer-by-layer, pixel-by-pixel) formation of a three-dimensional object. Various AM processes begin with disparate materials such as 1) Polymer-mixtures in stereolithography (SLA), embedded 3D printing (e3DP), and digital light-processing (DLP) 3D printing, 2) Thermoplastic filaments in fused deposition modeling (FDM), 3) Powders in selective laser sintering (SLS), selective laser melting (SLM), and electron beam melting and 4) Sheets in laminated object manufacturing (LOM) [1], [2], [3]. Some polymers involved in the first category are highly viscous, pseudoplastic fluids. On being poured in bulk into the fabrication space, gravitational forces prove to be inadequate to ensure proper flow resulting in an uneven polymer-air interface. Figure 1 illustrates this behavior by contrasting the air-polymer interfaces of fluids with low and high viscosities. In DLP and SLA techniques, a flat interface is essential before photo-polymerization to ensure uniform exposure. For SLA processes, the recommended upper-limit for the dynamic viscosity, μ, is 3000 $mPa.s$ to ensure uniform layer re-coating [4]. Traditionally, additives are added to these polymers to lower the value of μ at the cost of altering the mechanical properties of the cured material [5]. In e3DP, a high initial viscosity and strong pseudoplastic properties of the reservoir fluid are essential for satisfactory prints, restricting the use of such additives. Manual methods such as wiper/blade systems can be used to spread these materials uniformly throughout the fabrication space. However, these methods are unreliable and can lead to undesirable porosity in the cured part.

The application of longitudinal and transverse vibrations has been shown to lower the apparent viscosities and increase flow rates through pipes carrying pseudoplastic fluids [6, 7]. In

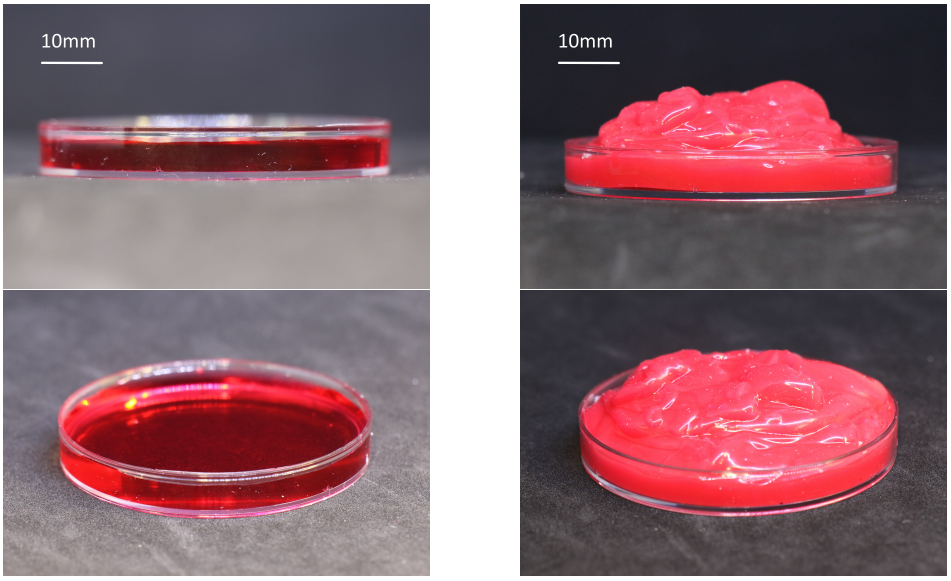

(a) (b)

Figure 1: Air-polymer interface formed due to (a) Water ($\mu_0 = 8.89 \times 10^{-4}\ Pa \cdot s$ at $25°C$), and (b) Platinum-cured silicone, Ecoflex 00-30 reservoir ($\mu_0 = 5.24 \times 10^{2}\ Pa \cdot s$ at $25°C$) [8]

this study, a similar physical principle is explored to achieve a flat air-polymer interface by applying an oscillatory shear stress using a vibrating actuator. The oscillatory shear stresses generated are shown to lower the apparent viscosity of a shear-thinning polymer, facilitating its flow within the fabrication-space. A fluid rheology model is presented to predict the parameters necessary to maximize the shearing-effect for an arbitrary pseudoplastic polymer. Experiments are also performed to demonstrate the efficacy of the proposed method of viscosity control for applications in e3DP in particular, but the method is applicable to any additive-manufacturing process involving shear-thinning polymers.

Fluid Rheology Control

Sinusoidal vibrations of amplitude, A, and angular velocity, ω, are used to generate variable shear rates and control the applied stress on a fluid. In a power law fluid, the relationship between the shear rate, $\dot{\gamma}$, and the resulting instantaneous fluid viscosity (i.e. apparent viscosity), $\mu_{apparent}$, is governed by the relations,

$$\tau = \mu_0(\dot{\gamma})^N \qquad \mu_{apparent} = \mu_0(\dot{\gamma})^{N-1} \tag{1}$$

where τ is the shear stress applied on the fluid, μ_0 is the viscosity at zero shear, and N is an empirically determined parameter. For a given fluid, we wish to identified the appropriate shear rate, $\dot{\gamma}$, to reach a target dynamic-viscosity, $\mu_{apparent} = \mu_{target}$, low enough for the fluid to settle down due to its own hydrostatic pressure. For a reservoir of non-Newtonian fluid, as shown in Figure 2, the force balance in x and y directions on an infinitesimally small element in the bulk of the fluid is given by,

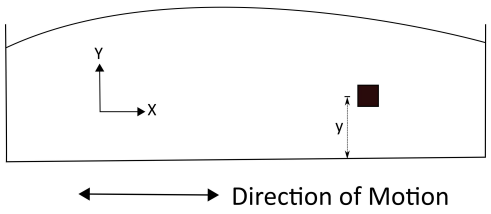

Figure 2: Schematic of theoretical model for rheology control of shear-thinning polymers.

$$\frac{\partial \tau_{xx}}{\partial x} + \frac{\partial \tau_{xy}}{\partial y} + \rho(g_x) = \rho \frac{dv_x}{dt} \tag{2a}$$

$$\frac{\partial \tau_{yx}}{\partial x} + \frac{\partial \tau_{yy}}{\partial y} + \rho(g_y) = \rho \frac{dv_y}{dt} \tag{2b}$$

where τ_{xx} and τ_{xy} represent the shear stresses in x and y directions respectively and ρ, v_x, and v_y denote the specific gravity and velocities of the fluid in x and y directions. The shear rate, $\dot{\gamma}$, in terms of the fluid column height, h, at any point y above the bottom of the container is given by,

$$\dot{\gamma} = \left[\frac{\rho}{\mu_0} (h-y) A\omega^2 \sin(\omega t) \right]^{\frac{1}{N}} \tag{3}$$

The acceleration, $g = A\omega^2$, required to attain μ_{target} of any specific fluid to ensure that fluid flows and flattens its surface due to its own hydrostatic pressure is then given by,

$$g = \left(\frac{1}{\rho(h-y)} \right) \left(\frac{1}{\mu_0} \right)^{\frac{1}{N-1}} \left(\mu_{target} \right)^{\frac{N}{N-1}} \tag{4}$$

For pseudoplastic fluids $(N < 1)$, there is an inverse relationship between g and μ_{target}. Equation (4) doesn't take into account the relaxation time of the fluid on a molecular level characterized by the Deborah Number (De), the ratio of t_c, the relaxation time, and t_p, the time of observation for the fluid. At higher frequencies, the smaller values of t_p for any fluid prevents any subsequent decrease in the viscosity of the fluid. This limiting frequency differs for each fluid and can be determined experimentally.

Experimental Validation

Material Preparation

A platinum-cured liquid silicone rubber was prepared by adding 2wt% SLO-JO and 1wt% Thivex to Part-B of Ecoflex 00-30, followed by addition of Part-A of Ecoflex 00-30 (Smooth-On Inc). The polymer mixture was mixed in a planetary mixer (ARE-310, THINKY; Tokyo,

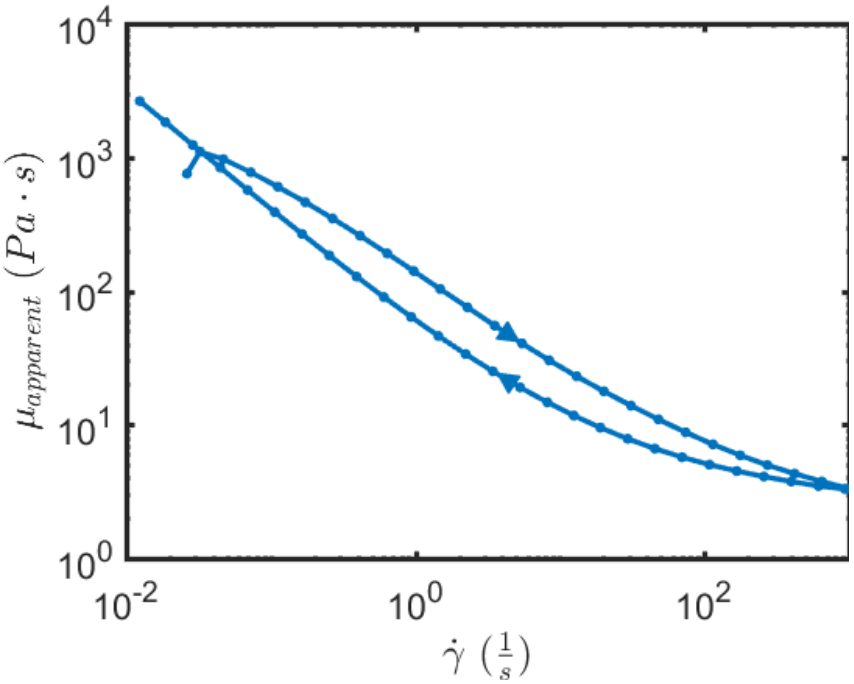

Figure 3: Apparent viscosity versus shear rate of modified Ecoflex 00-30 liquid silicone rubber. The measurements highlight the shear thinning and thixotropic properties of the fluid.

Japan) at 2000 rpm for 2 minutes followed by degassing at 2200 rpm for 1 minute [8]. This formulation was chosen as a typical reservoir material used for embedded 3D printing in our lab. The rheological properties of the uncured reservoir were measured using a rheometer (Discovery HR2, TA Instruments; New Castle, DE; 40 mm parallel plate, gap width = 500μm) by increasing the shear rate from 0 to 10^3 $1/s$ and then decreasing it back to the initial value over a span of 2 minutes. The results are shown in Figure 3. The presence of a hysteresis loop reveals significant thixotropy changes over timescales of tens of seconds.

A power-law curve fitted to the rheology characteristics of Ecoflex 00-30 polymer mixture yields $\mu_0 = 137.79$ *Pa.s*, and $N = 0.395$. Equation 4 was used to predict $\mu_{apparent}$ at different depths below the fluid-air interface $(h-y) = 5, 15$, and 25 *mm*. These calculated values are plotted in Figure 4. The static dynamic viscosities of two common fluids, unmodified Ecoflex 00-30 and honey ($\mu_0 = 3$, and 10 *Pa.s* respectively) are provided for comparison.

Based on observations that unmodified Ecoflex 00-30 readily flows to fill most molds and form a flat fluid-air interface, the model predicts that accelerations greater than ≈ 50 m/s^2 will shear thin the modified reservoir material sufficiently to induce satisfactory mold filling.

Extrusion Experiment

The experimental setup is shown in Figure 5. A controlled acceleration, g, was applied using a shaker (U56001, 3B Scientific; Hamburg, Germany) driven by a function generator (FG100, 3B Scientific; Hamburg, Germany). The applied acceleration, g, was measured using an accelerometer (EVAL-ADXL326Z, Analog Devices; Norwood, MA). All measured acceler-

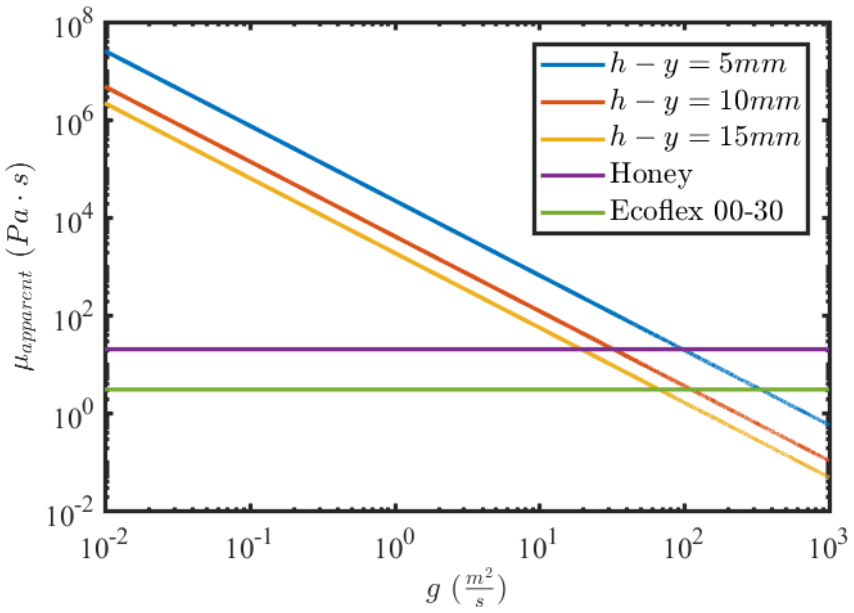

Figure 4: Predicted $\mu_{apparent}$ verus applied acceleration g at various reservoir depths.

ation values fit a sinusoidal profile with coefficient of determination, $R^2 > 0.98$. Corresponding amplitude values were calculated from acceleration measurements using the relation $A = g/\omega^2$.

To quantify the the viscosity reduction caused by an applied oscillatory shear stress, we measured the mass flow rate of the aforementioned modified Ecoflex 00-30 mixture from a container with a 2 *mm* diameter circular aperture with and without an applied oscillatory acceleration input. For each run of the experiment, the container was filled with uncured liquid silione rubber mixture and sealed. The sealed container was attached to the shaker and a constant driving pressure of 14 *kPa* was applied through a pneumatic fitting. The applied pneumatic pressure sets up a flow of liquid rubber through the aperture and onto a receptacle placed on an electronic balance. The mass of the fluid collected was measured in real-time as the experiment progressed.

During control runs, the container was held stationary. During the treatment condition, the

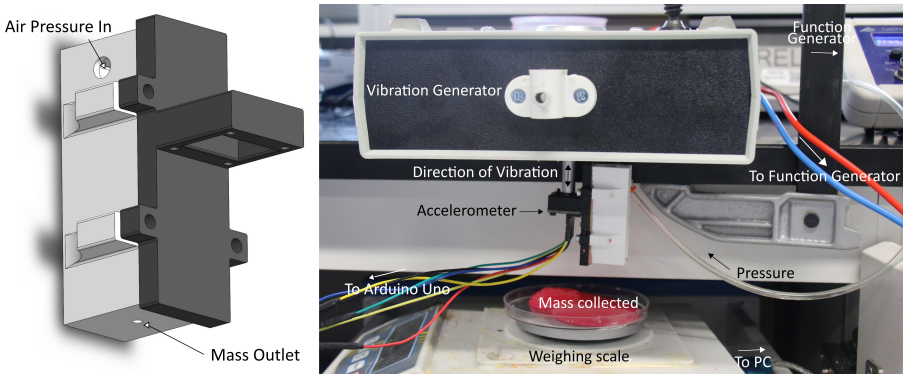

Figure 5: Photograph of extrusion experiment setup and CAD rendering of the reservoir container.

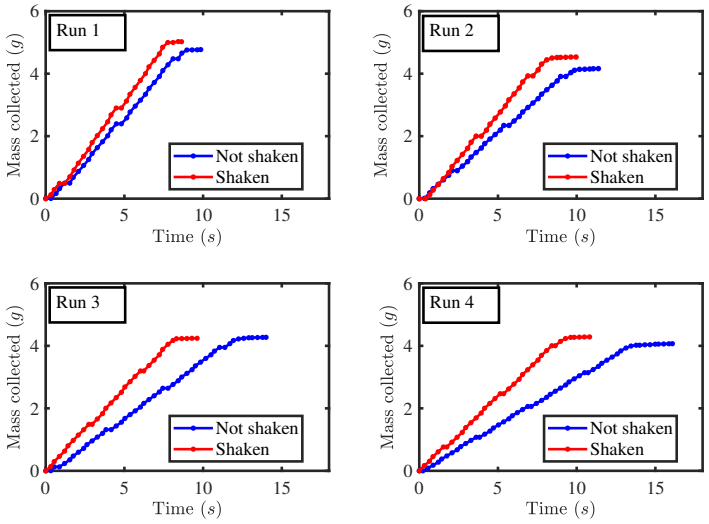

Figure 6: Mass of liquid rubber collected over time.

shaker moves the container vertically at $45Hz$, applying a peak acceleration value of $40.95\ {}^{m}/_{s^2}$. A total of 4 measurements were made for the control condition at an interval of 5 minutes, followed by preparation of a fresh batch of material for 4 measurements for the treatment condition. The results are shown in Figure 6. Mass data is grouped by run number (i.e. the number of experiment runs since the current batch of material was prepared) to aid visual distinction between the effect of real-time oscillatory shear and thixotropy. Figure 6 shows a rapid reduction in average mass flow rate over run number for samples subjected to the control condition. In contrast, samples subjected to the shaking treatment not only retained a more consistent mass flow rate over run number, but experienced a consistently higher mass flow rate compared to the control sample sharing the same run number.

We postulate that the observed pattern is caused by the combined effect of real-time shear thinning in response to the applied oscillatory stress and thixotropy. Each new batch of material experiences significant shear during the planetary mixing process, causing a temporary drop in $\mu_{apparent}$ that gradually recovers over the (as yet unmeasured) thixotropic time scale of the material. As run number progresses, as long as the material undergoes no further shearing, $\mu_{apparent}$ gradually recovers to its steady-state value, causing the control samples to exhibit a falling mass flow rate over time. This time-dependent fall in flow rate is much less marked in samples subjected to the externally applied oscillation during extrusion, because this oscillatory shear stress induces real-time shear thinning in the material, counteracting the thixotropic recovery. It is worth nothing that the samples subjected to shaking retained a measurable, albeit slower, decay in mass flow rate over increasing run numbers. This phenomenon may be explained by permanent changes in material viscosity due to cure progress, incomplete masking of the thixotropic effect by real-time oscillation due to relatively much higher shear rates applied during planetary mixing, or a combination of these two effects.

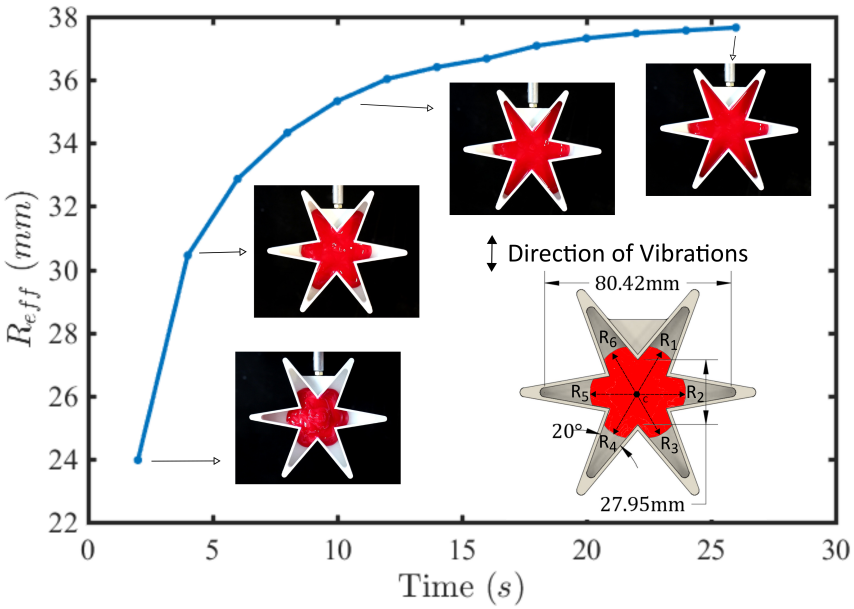

Figure 7: Mean effective radius of Ecoflex 00-30 as a function of time in a star-shaped mold.

Application Example

In order to test the effects of rheology control in a realistic scenario, a 15 *mm*-deep star-shaped mold was used to simulate the complexities (i.e. sharp corners) in a typical fabrication environment. The mold was mounted to the shaker, and 10 grams of the reservoir material was placed in a mound at the center of the mold, and vibrated at 53.3 $^{m}/_{s^2}$ of acceleration, 30 Hz for 2 seconds at a time along the direction indicated in Figure 7. In order to equalize the shear history of the materials used and minimize the confounding effect of thixotropy, the liquid silicone rubber was agitated on a vortex mixer immediately prior to loading into molds.

The fluid front ascended in each ”leg” of the star and the mean effective radius, R_{eff}, was calculated at each time point using $\frac{1}{6}(\sum_{i=1}^{6} R_i)$ where R_i is the distance of the fluid front in each ‘leg’ from the center of the mold, C. The lack of flow in the ‘legs’ perpendicular to the direction of vibration can be explained by a dearth of shearing surface, thus showing that the observed flow is primarily due to the effect of real-time oscillatory shear instead of thixotropy.

Conclusions

The application of an oscillatory shear-stress is shown to reduce the local dynamic viscosity, μ, of a shear-thinning fluid and this approach can be used to ease polymer flow in the fabrication space. The parameters influencing the process are the viscosity at zero shear (μ_0), the applied acceleration, g, and the shear thinning behavior of the fluid defined by a power law coefficient N. Subsequent work is required to determine the effects of different waveforms (e.g. square, sawtooth, and triangle waves) on the fluid-flow along with further development of a device based on the proposed approach for additive manufacturing applications.

Acknowledgements

We acknowledge the support of the SUTD Digital Manufacturing and Design (DManD) Centre which is supported by the National Research Foundation Singapore.

References

[1] K. V. Wong and A. Hernandez, "A Review of Additive Manufacturing," *ISRN Mechanical Engineering*, vol. 2012, pp. 1–10, 2012. [Online]. Available: http://www.hindawi.com/journals/isrn/2012/208760/

[2] J. Gardan, "Additive manufacturing technologies: State of the art and trends," *International Journal of Production Research*, vol. 54, no. 10, pp. 3118–3132, 2016. [Online]. Available: http://dx.doi.org/10.1080/00207543.2015.1115909

[3] F. Calignano, D. Manfredi, E. P. Ambrosio, S. Biamino, M. Lombardi, E. Atzeni, A. Salmi, P. Minetola, L. Iuliano, and P. Fino, "Overview on additive manufacturing technologies," *Proceedings of the IEEE*, vol. 105, no. 4, pp. 593–612, 2017.

[4] M. L. Griffith and J. W. Halloran, "Freeform Fabrication of Ceramics via Stereolithography," pp. 2601–2608, 2005.

[5] S. C. Ligon, R. Liska, J. Stampfl, M. Gurr, and R. Mülhaupt, "Polymers for 3D Printing and Customized Additive Manufacturing," *Chemical Reviews*, vol. 117, no. 15, pp. 10 212–10 290, 2017.

[6] N. S. Deshpande and M. Barigou, "Vibrational flow of non-Newtonian fluids," *Chemical Engineering Science*, vol. 56, pp. 3845–3853, 2001.

[7] S. Shin and J. H. Lee, "Characteristics of shear-thinning fluid flow under traversal vibration," *Japanese Journal of Applied Physics, Part 1: Regular Papers and Short Notes and Review Papers*, vol. 42, no. 3, pp. 1363–1367, 2003.

[8] J. T. Muth, D. M. Vogt, R. L. Truby, Y. Menguc, D. B. Kolesky, R. J. Wood, and J. A. Lewis, "Embedded 3D printing of strain sensors within highly stretchable elastomers," *Advanced Materials*, vol. 26, no. 36, pp. 6307–6312, 2014.